Original Article

OPEN

KAT7 contributes to ponatinib-induced hypertension by promoting endothelial senescence and inflammatory responses through activating NF-κB signaling pathway

Liang-Liang Tang[a], Xin-Yu Xu[a], Mei Zhang[b,c], Qi Qin[a], Rong Xue[a], Shuai Jiang[a], Xu Yang[a], Chen Liang[b,c], Qiu-Shi Wang[b,c], Chang-Jiang Yu[a], and Zhi-Ren Zhang[a,b,c]

Background and purpose: Ponatinib, a tyrosine kinase inhibitor (TKI) leads to hypertension; however, the mechanisms remain elusive. We aimed to investigate whether lysine acetyltransferase 7 (KAT7), a key regulator of cellular senescence that is closely associated with cardiovascular diseases, involves in ponatinib-induced hypertension.

Methods and results: After administering ponatinib to Sprague–Dawley (SD) rats for 8 days, we measured blood pressure, vasodilation, and endothelial function using tail-cuff plethysmography, isometric myography, and the Total NO Assay kit, respectively. The results indicated that ponatinib increased blood pressure, impaired endothelium-dependent relaxation (EDR), and caused injury to endothelial cells in SD rats. Furthermore, PCR and Western blot experiments demonstrated an upregulation of KAT7 expression in rat mesenteric artery endothelial cells (MAECs) following ponatinib treatment. To further study the role of KAT7 in ponatinib-induced hypertension, we divided the SD rats into four groups: control, ponatinib, WM-3835 (a KAT7 inhibitor), and ponatinib plus WM-3835. Notably, WM-3835 administration significantly improved ponatinib-induced hypertension and EDR dysfunction in SD rats. Mechanistically, over-expression of KAT7 (OE-KAT7) in MAECs led to cellular senescence and inflammation, phenomena that were also observed in the mesenteric arteries of ponatinib-treated rats and in MAECs exposed to ponatinib. However, WM-3835 mitigated these detrimental effects in both *in vivo* and *in vitro* experiments. Additionally, both OE-KAT7 and ponatinib treatment induced H3K14 acetylation (H3K14ac), with OE-KAT7 also elevating the recruitment of the H3K14ac to the p21 promoter. Moreover, BAY 11-7085, a nuclear factor (NF)-κB inhibitor, potently alleviated the accumulation of IL-6 and IL-8, as well as endothelial cell senescence induced by ponatinib and KAT7 overexpression.

Conclusion: Our data indicate that ponatinib-induced elevation of KAT7 led to endothelial cells senescence and inflammatory responses through H3K14 acetylation and NF-κB signaling pathway, subsequently caused vasotoxicity and hypertension.

Keywords: hypertension, lysine acetyltransferase 7, nuclear factor-κB, ponatinib, vascular toxicity

Abbreviations: BAY, BAY 11-7085; EDR, endothelium-dependent relaxation; IL-6, interleukin-6; IL-8, interleukin-8; KAT7, lysine acetyltransferase 7; MA, mesenteric artery; MAECs, mesenteric artery endothelial cells; NC, negative control; NF-κB, nuclear factor of kappa light polypeptide gene enhancer in B cells; NO, nitric oxide; OE, overexpression; PCR, polymerase chain reaction; PON, ponatinib; SASP, senescent-associated secretory phenotype; SD, Sprague–Dawley; TKIs, tyrosine kinase inhibitors

INTRODUCTION

Ponatinib, marketed as Iclusig, is a third-generation tyrosine kinase inhibitor (TKI). It has been approved by the US Food and Drug Administration for the treatment of chronic myeloid leukemia and Philadelphia chromosome-positive acute lymphoblastic leukemia in patients, who are resistant to or intolerant of prior TKI therapy [1,2]. One of the most significant aspects of ponatinib is its exceptional efficacy against the "gatekeeper

Journal of Hypertension 2025, 43:827–840

[a]Department of Pharmacy and Cardiology, Harbin Medical University (HMU) Cancer Hospital, Institute of Metabolic Disease, Heilongjiang Academy of Medical Science, Heilongjiang Key Laboratory for Metabolic Disorders and Cancer related Cardiovascular Diseases, [b]Department of Cardiology and Critical Care Medicine, the First Affiliated Hospital of HMU, NHC Key Laboratory of Cell Transplantation, Key Laboratories of Education Ministry for Myocardial Ischemia Mechanism and Treatment and [c]State Key Laboratory of Frigid Zone Cardiovascular Diseases (SKLFZCD), HMU, Harbin 150081, China

Correspondence to Zhi-Ren Zhang, MD, PhD, Department of Cardiology and Critical Care Medicine, NHC Key Laboratory of Cell Transplantation. The First Affiliated Hospital of Harbin Medical University, No. 23 Youzheng Street, Nangang District, Harbin, 150001, China. E-mail: zhirenz@163.com or zhirenz@hrbmu.edu.cn

Received 14 July 2024 **Revised** 18 December 2024 **Accepted** 16 January 2025

DOI:10.1097/HJH.0000000000003979

mutation" ABL T315I [3]. However, ponatinib has been associated with serious adverse vascular events and cardiotoxicity, including hypertension (68%), thrombosis (16.3%), vascular occlusion events (6%), and heart failure (3–15%) [4–7]. Hypertension is a common adverse event in patients receiving ponatinib and is a significant risk factor for cardiovascular disease [6,8,9]. These adverse effects have limited the widespread clinical application of ponatinib [10]. It is believed that these adverse vascular events are due to off-target effects, but the molecular mechanisms underlying ponatinib-induced hypertension remain largely unknown.

Previous studies have demonstrated that ponatinib may induce vascular damage by directly targeting vascular endothelial cell [11], as its targets are expressed on the surface of endothelial cells. Endothelial dysfunction caused by ponatinib disrupts the balance of vascular homeostasis and may explain the development of hypertension and other adverse vascular events. Additionally, many TKIs including ponatinib, can induce cellular senescence in both cancerous cells and noncancerous cells [11–15]. While senescence is thought to prevent the uncontrolled proliferation of damaged cells, it also promotes the expression of inflammatory cytokines, leading to an inflammatory phenotype known as the senescence-associated secretory phenotype (SASP) [16,17]. Endothelial cells senescence is considered a crucial risk factor for endothelial dysfunction and vascular damage [18]. Based on these findings, we hypothesize that the vasotoxicity and hypertension associated with ponatinib may be linked to its induction of endothelial cell senescence.

Lysine acetyltransferase 7 (KAT7), also known as HBO1 or MYST2, is a member of the MYST family. Its primary function is to acetylate lysine 14 on histone 3 (H3K14ac). Recent studies have highlighted the significant role of KAT7 in regulating cellular senescence [19,20]. The inactivation or depletion of KAT7 has been shown to alleviate various characteristics of aging and extend lifespan in animal models [19,21,22]. However, there is currently limited evidence regarding KAT7′ role in vascular aging or the regulation of blood pressure.

In our study, we found that the administration ponatinib led to an increase in blood pressure and impaired endothelium-dependent relaxation in Sprague–Dawley rats. These effects were mitigated by WM-3835, a KAT7 inhibitor. Mechanistically, ponatinib elevated the expression of KAT7, which subsequently led to endothelial senescence, inflammation, and dysfunction through acetylate H3K14 and activation of nuclear factor (NF)-κB signaling pathway. In summary, our study elucidates the potential mechanisms underlying ponatinib-induced hypertension.

MATERIALS AND METHODS

Animals and experiment protocols

All animal care and experimental procedures were approved by the Animal Research Ethical Committee of Harbin Medical University (HMU). All studies involving animals conformed to the ARRIVE guidelines for reporting animal research [23]. Male Sprague–Dawley rats weighing between 180 and 200 grams were purchased from the animal center of the Second Affiliated Hospital of HMU (Harbin, China). The rats were randomly assigned to four groups: control, ponatinib (HY-12047, MedChemExpress, United States), WM-3835 (HY-134901, MedChemExpress, United States), and ponatinib + WM-3835. Ponatinib was dissolved in DMSO (D2650, Sigma, United States), diluted with corn oil (C116025, Aladdin, China), and administered intragastrically at a dosage of 6 mg/kg/day. WM-3835 was also dissolved in DMSO, diluted with corn oil, and administered via intraperitoneal injection at a dosage of 10 mg/kg/day. After 8 days, the animals were euthanized, and mesenteric arteries (MAs) were collected and prepared for subsequent experiments.

Blood pressure measurement

The systolic blood pressure (SBP) of rats was measured on days 0 and 8 using tail-cuff plethysmography (CODA, 20310, Kent Scientific Corporation, United States). The rats were restrained in a tube and put on a heating pad preheated around 35°C. Blood pressure was recorded 15 times, and the average of six values was calculated after discarding the extreme values.

Primary cultured rat mesenteric artery endothelial cells and groups

Mesenteric artery endothelial cells (MAECs) were isolated and cultured following established protocols [24,25]. Briefly, male SD rats were euthanized, and the entire mesentery was excised and cut into several parts. The tissue was then digested using 0.2% type IA collagenase at 37°C for 50 min. The digestion was terminated by adding DMEM with high glucose, supplemented with 20% fetal bovine serum, 1% penicillin, and 1% streptomycin. Filtrated liquid was centrifuged at 1200 g for 5 min and supernatant was aspirated. The cells were seeded in a Petri dish and incubated in a humidified atmosphere containing 5% CO_2. These primary isolated cells were used for experiments without further passage.

To determine the effect of KAT7 on ponatinib-induced senescence and inflammation in MAECs, the cells were divided into four groups: control, ponatinib (100 nM), WM-3835 (100 nM) and a combination of ponatinib (100 nM) and WM-3835 (100 nM). The cells receiving indicated treatment were cultured for 24 h.

To investigate the role of NF-κB signaling pathway in ponatinib- or KAT7 overexpression (OE)-induced senescence and inflammation in MAECs, the cells were transfected with a KAT7 overexpression plasmid or an empty vector serving as a negative control (NC). Subsequently, the cells were divided into five groups: NC, NC + ponatinib (100 nM), OE-KAT7, NC + ponatinib (100 nM) + BAY 11-8075 (5 μM; HY-10257, MedChemExpress, United States), and OE-KAT7 + BAY 11-8075 (5 μM). The cells receiving indicated treatment were cultured for 24 h.

Western blot

Protein samples were prepared from MAECs and MAs. Some MAs were pulled through the lumen of the vessel using a metal wire and gently rolled to remove the endothelial layer for denuding endothelial cells. The absence of the endothelium was confirmed by assessing eNOS expression. The samples were separated by SDS-polyacrylamide gel and then transferred to a nitrocellulose membrane. The

membranes were then blocked with either 5% skim milk or 5% bovine serum albumin in Tris-buffered saline for 1 h. Then, the membranes were incubated overnight at 4°C with the primary antibody: anti-KAT7 (1 : 1000 dilution, 13751-1-AP, Proteintech, United States), anti-p21 (1 : 1,000 dilution, ab109199, Abcam, United Kingdom), anti-phospho-p65 (Ser536, 1 : 1000 dilution, 3033S, CST, United States), anti-p65 (1 : 1000 dilution, 8242S, CST, United States), anti-Gapdh (1 : 10 000 dilution, ab8245, Abcam, United Kingdom), anti-H3K14ac (1 : 1000 dilution, 7627S, CST, United States), anti-H3K34ac (1 : 100 dilution, A18154, ABclonal, China) and anti-H3 (1 : 2000 dilution, 4499T, CST, United States). Incubated membranes with IRDye 800CW-conjugated goat antirabbit (1 : 10 000, P/N 926-32211, LI-COR, United States) or IRDye 680RD-conjugated goat antimouse (1 : 10 000, P/N 926-68070, LI-COR, United States) for 1 h at room temperature. Protein bands were detected with Odyssey infrared imaging system (LI-COR) and analyzed by using Image Studio Software.

Quantitative real-time PCR

Total RNA from MAECs or MAs was extracted, and cDNAs were synthesized using a reverse transcription kit (4368814, Applied Biosystems, United States). qRT-PCR was conducted using the SYBR Green PCR Core Reagents Kit (R323-01, Vazyme Biotech, China). The transcription levels of mRNAs were measured using the comparative CT method, normalized to Gapdh, and calculated using the $2^{-\Delta\Delta CT}$ method. mRNA expression levels were determined using the following primers: KAT7 forward (5′-GCACTGAGGAACCCGCCTAT-3′), KAT7 reverse (5′-ACCGCCTGTTCCGTTTCAGA-3′), IL-6 forward (5′-GTTGCCTTCTTGGGACTGAT-3′), IL-6 reverse (5′-TGTGTAATTAAGCCTCCGACT-3′), IL-8 forward (5′-GGTAAAGTCCGTAAGTCGTAGTAC-3′), IL-8 reverse (5′-AGTTAACGTGGAGGTACCGTA-3′), Gapdh forward (5′-CAACTTTGGCATTGTGGAAGG-3′), Gapdh reverse (5′-ACACATTGGGGGTAGGAACAC-3′), p21 promoter forward (5′-AGTGGATTCAAACATATGAGCCACT-3′) and p21 promoter reverse (5′-CCCTCCATCCCCCAAGGCCCTG-3′).

Cell viability measurement

The viability of MAECs was measured with Cell Counting Kit-8 (CCK-8, CK-04, DOJINDO Laboratories, Japan) according to the manufacturer's instructions.

Nitric oxide measurement

The nitric oxide (NO) production in MAs was determined by the Total NO Assay Kit (S0021S, Beyotime Company, China) according to the manufacturer's instructions.

Vasodilation function in mesenteric artery

The vasodilatory function of isolated MA was measured by isometric myography (Danish Myo Technology, Aarhus, Denmark), as previously described [24–26]. Second-order MAs isolated from SD rats were cut into 2 mm ring segments and mounted on a wire myograph in a physiological salt solution containing 95% O_2 and 5% CO_2 at 37°C. After stabilization, the rings were adjusted to optimal tension and stabilized again for 30 min. MA rings were precontracted with phenylephrine (Phe, 10 mM; P6126-5G, Sigma-Aldrich, United States), and vascular responses to varying concentrations of acetylcholine (Ach, concentrations ranging from 0.1 nM to 10 μM; A6625-25G, Sigma-Aldrich, United States) and nitroglycerin (NTG, concentrations ranging from 0.1 nM to 10 μM; 100236-201702, National Institutes for Food and Drug Control, China) were recorded. Some MAs were obtained from SD rats treated with ponatinib, with or without WM-3835. For *in vitro* experiments, MA rings from normal SD rats were incubated with either 100 nM ponatinib, 100 nM WM-3835, or a combination of 100 nM ponatinib and 100 nM WM-3835 for 3 h.

Cell senescence staining

Senescence of MAECs was determined by staining the senescence-associated β-galactosidase (SA-β-gal) with the Senescence β-galactosidase Staining Kit (C0602, Beyotime Company, China) according to the manufacturer's instructions.

Synthesis and transfection of overexpression plasmid

The overexpression plasmid of KAT7 was designed and synthesized by Sangon Biotech (Shanghai, China). Plasmids were transfected into MAECs using Lipofectamine 3000 reagent (L3000015, Invitrogen, United States) according to the manufacturer's instructions.

Chromatin immunoprecipitation-qPCR assays

The binding of KAT7 and H3K14ac to the p21 promoter was analyzed by chromatin immunoprecipitation (ChIP) assay. MAECs transfected with either the KAT7 overexpression plasmid or an empty vector were subjected to the ChIP assay using the ChIP Assay Kit (p2078, Beyotime Biotechnology, Shanghai, China) according to the manufacturer's instructions. The cell lysates were then immunoprecipitated with anti-KAT7, anti-H3K14ac, or immunoglobulin G (IgG) antibodies. The DNA segments were purified using a DNA Purification Kit (D0033, Beyotime Biotechnology, Shanghai, China) and subsequently utilized for qPCR analysis.

Statistics

Data were expressed as mean ± SEM. Student's *t*-test was employed to analyze differences between two groups. One-way or two-way ANOVA with post hoc Tukey's test was employed to analyze differences among multiple groups using GraphPad Prism 6 software (GraphPad Software, Inc., San Diego, United States). $P < 0.05$ was considered statistically significant.

RESULTS

Ponatinib induces hypertension and impairs endothelium-dependent relaxation in Sprague–Dawley rats

Ponatinib induces a high incidence of hypertension; however, the mechanisms by which ponatinib-induced hypertension remain to be elucidated. We aimed to investigate these mechanisms using SD rats as an experimental model. As shown in Fig. 1a, ponatinib administration led to a

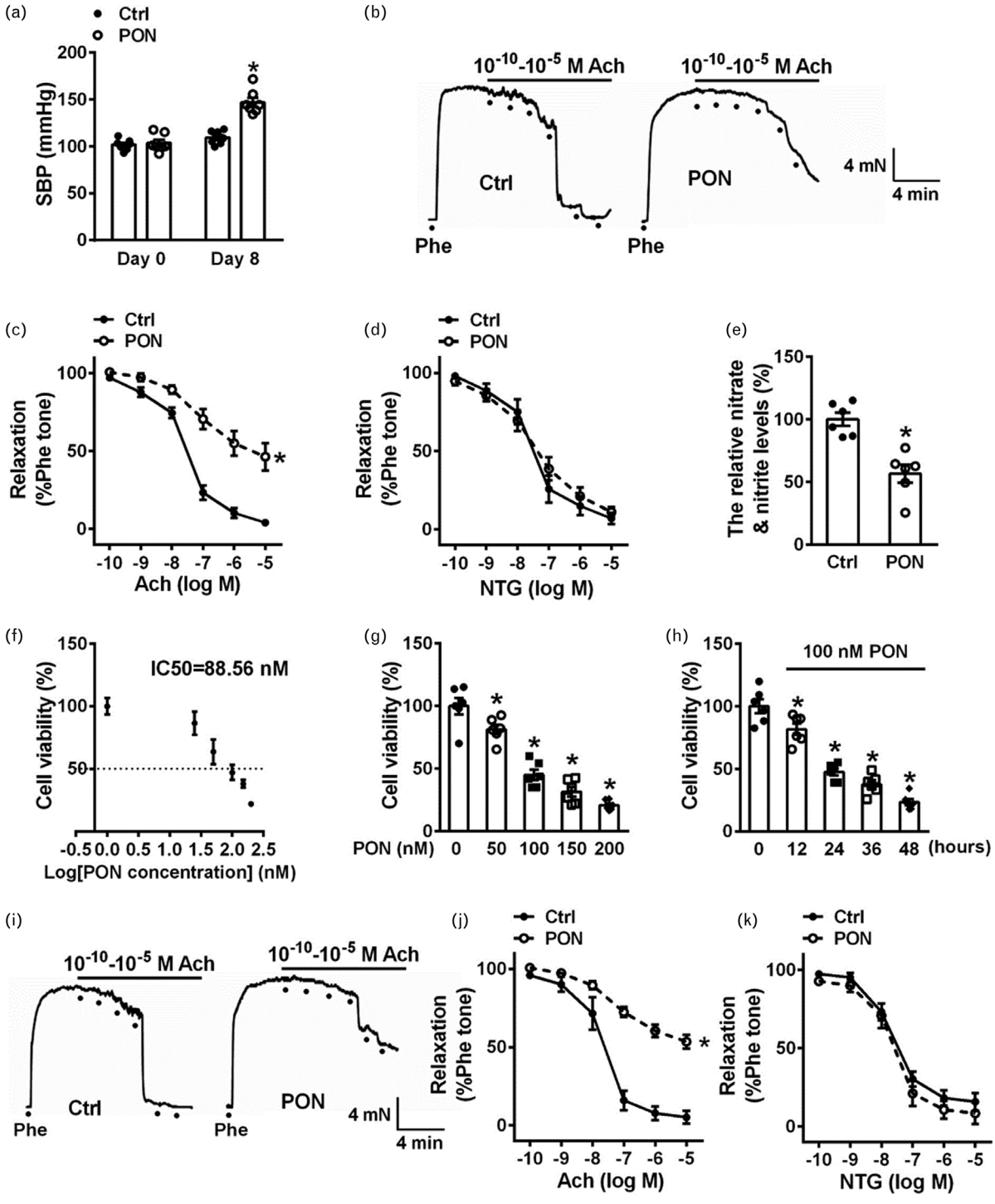

FIGURE 1 Ponatinib leads to an increase in blood pressure and an impaired EDR. (a) The systolic blood pressure (SBP) of control and ponatinib administration rats were measured by the noninvasive tail-cuff method. The data are means ± SEM, $n = 7$ per group. $^*P < 0.05$ versus control. (b) Representative traces obtained by wire myography and (c) summarized data of Ach-induced relaxation of the MA rings from the control rats or ponatinib administration rats, followed by precontracting with 10 μM Phe before application of 0.1 nM to 10 μM Ach. The data are means ± SEM, $n = 6$ per group. $^*P < 0.05$ versus control. (d) Summarized percentage changes of endothelium-independent relaxation in response to different concentrations of NTG (0.1 nM to 10 μM) in MA rings from each indicated group (raw data not shown). The data are means ± SEM, $n = 6$ per group. (e) The concentrations of nitrate and nitrite measured in MAs isolated from the two groups rats as mentioned above. The data are means ± SEM, $n = 6$ per group. $^*P < 0.05$ versus control. (f) IC50 value was determined by CCK-8 assay after exposure to increasing concentration of ponatinib (0, 25, 50, 100, 150, 200 nM) for 24 h. The data are means ± SEM, $n = 6$ per group. (g) Concentration-dependent effect of ponatinib on MAECs viability. MAECs were incubated for 24 h with ponatinib from 50 nM to 200 nM. Cell viability was determined by CCK-8 assay as a percentage of control. The data are means ± SEM, $n = 6$ per group. $^*P < 0.05$ versus control. (h) Time-dependent effect of ponatinib on MAECs viability. MAECs were incubated with 100 nM ponatinib for various time (0, 12, 24, 36, 48 h). Cell viability was determined by CCK-8 as a percentage of control. The data are means ± SEM, $n = 6$ per group. $^*P < 0.05$ versus control. (i) Representative traces obtained by wire myography and (j) summarized data of Ach-induced relaxation of the MA rings; the rings were under control condition or treated with 100 nM ponatinib for 3 h, followed by precontracting with 10 μM Phe before application of 0.1 nM to 10 μM Ach. The data are means ± SEM, $n = 6$ per group. $^*P < 0.05$ versus control. (k) Summarized percentage changes of endothelium-independent relaxation in response to different concentrations of NTG (0.1 nM to 10 μM) in MA rings from each indicated group (raw data not shown). The data are means ± SEM, $n = 6$ per group.

significant elevation in blood pressure compared to the control group.

Subsequently, we examined the impact of ponatinib on the relaxation of the mesenteric artery. Our results demonstrated that ponatinib administration significantly decreased Ach-induced EDR in the MA, indicating impaired vascular function (Fig. 1b, c). However, endothelium-independent relaxation induced by NTG was not affected in SD rats treated with ponatinib (Fig. 1d). Furthermore, we found a significant decrease in the concentration of nitrate and nitrite, which are precursors for NO production, following ponatinib administration (Fig. 1e). These findings suggest that ponatinib induces endothelial cell damage in SD rats.

To further investigate the effects of ponatinib on endothelial cells, we performed CCK-8 assay to assess the viability of MAECs following exposure to ponatinib. The half-maximal inhibitory concentration (IC50) of ponatinib for MAECs was calculated to be 88.56 nM (Fig. 1f). Thus, we utilized a concentration of 100 nM of ponatinib for the subsequent experiments. Consistent with our expectations, we found that ponatinib caused concentration-dependent and time-dependent damage to MAECs (Fig. 1g-h).

To corroborate these findings, we treated MAs isolated from normal SD rats with 100 nM ponatinib for 3 h and assessed the vascular tone. The results indicated that ponatinib decreased Ach-induced EDR in MAs, while NTG-induced endothelium-independent relaxation remained unaffected (Fig. 1i–k). Collectively, these findings suggest that ponatinib results in endothelial dysfunction in MAECs.

Ponatinib enhances the expression of KAT7 in mesenteric artery endothelial cells

It has been documented that KAT7 plays a crucial role in cellular processes; however, its specific involvement in vascular endothelial cells is not well studied. Here, endothelium-intact and endothelium-denuded mesenteric arteries were collected. Endothelial nitric oxide synthase (eNOS) was utilized as a marker to identify ECs within the MAs (Fig. 1a, b, Supplemental Digital Content, http://links.lww.com/HJH/C654). Our findings revealed that the expression level of KAT7 was significantly higher in ponatinib treated MA with ECs compared to those without ECs (Fig. 2a). Next, we isolated and cultured primary MAECs from normal SD rats for Western blot and PCR analysis. The data indicated that ponatinib treatment significantly elevated both protein expression and mRNA levels of KAT7 compared to control cells (Fig. 2b, c). Collectively, these results suggest that ponatinib upregulates KAT7 in vascular endothelial cells.

Inhibition of KAT7 alleviates ponatinib-induced hypertension and endothelium-dependent relaxation dysfunction in Sprague–Dawley rats

To investigate the role of KAT7 in ponatinib-induced hypertension and vasotoxicity, we conducted experiments to monitor blood pressure in conscious animals administered ponatinib, WM-3835, or a combination of both. Our findings revealed that the increase in blood pressure caused by ponatinib was significantly mitigated by the administration of WM-3835 (Fig. 3a). Additionally, WM-3835 provided protection against ponatinib-induced EDR dysfunction (Fig. 3b, c). However, none of the treatments (ponatinib, WM-3835, or the combination) affected endothelium-independent relaxation induced by NTG (Fig. 3d). Subsequently, we examined the effects of these treatments on NO production. Our data showed that the ponatinib-induced reduction in concentration of nitrate and nitrite was significantly reversed by the administration of WM-3835 in SD rats (Fig. 3e).

In addition, we treated MAs isolated from normal SD rat with ponatinib, WM-3835 or a combination of both for 3 h. The data showed that ponatinib impaired Ach-induced EDR

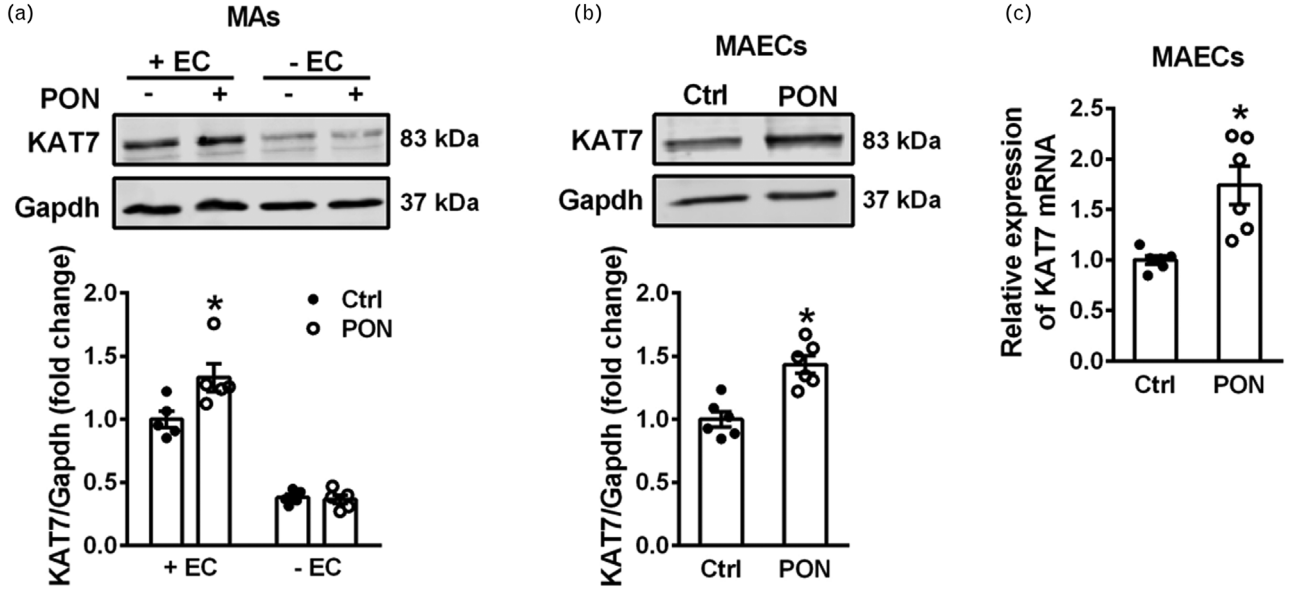

FIGURE 2 Ponatinib increases the expression levels of KAT7 in MAECs. (a) Western blot analysis (upper) and summarized data (lower) of KAT7 expression in MAs with or without endothelial cell (EC), following treatment with 100 nM ponatinib for 6 h. The data are means ± SEM, $n = 5$ per group. $^*P < 0.05$ versus control with EC. (b) Western blot analysis (upper) and summarized data (lower) of KAT7 expression in MAECs treated with or without 100 nM ponatinib for 24 h. The data are means ± SEM, $n = 6$ per group. $^*P < 0.05$ versus control. (c) PCR analysis of KAT7 mRNA levels in MAECs as treated above. The data are means ± SEM, $n = 6$ per group.$^*P < 0.05$ versus control.

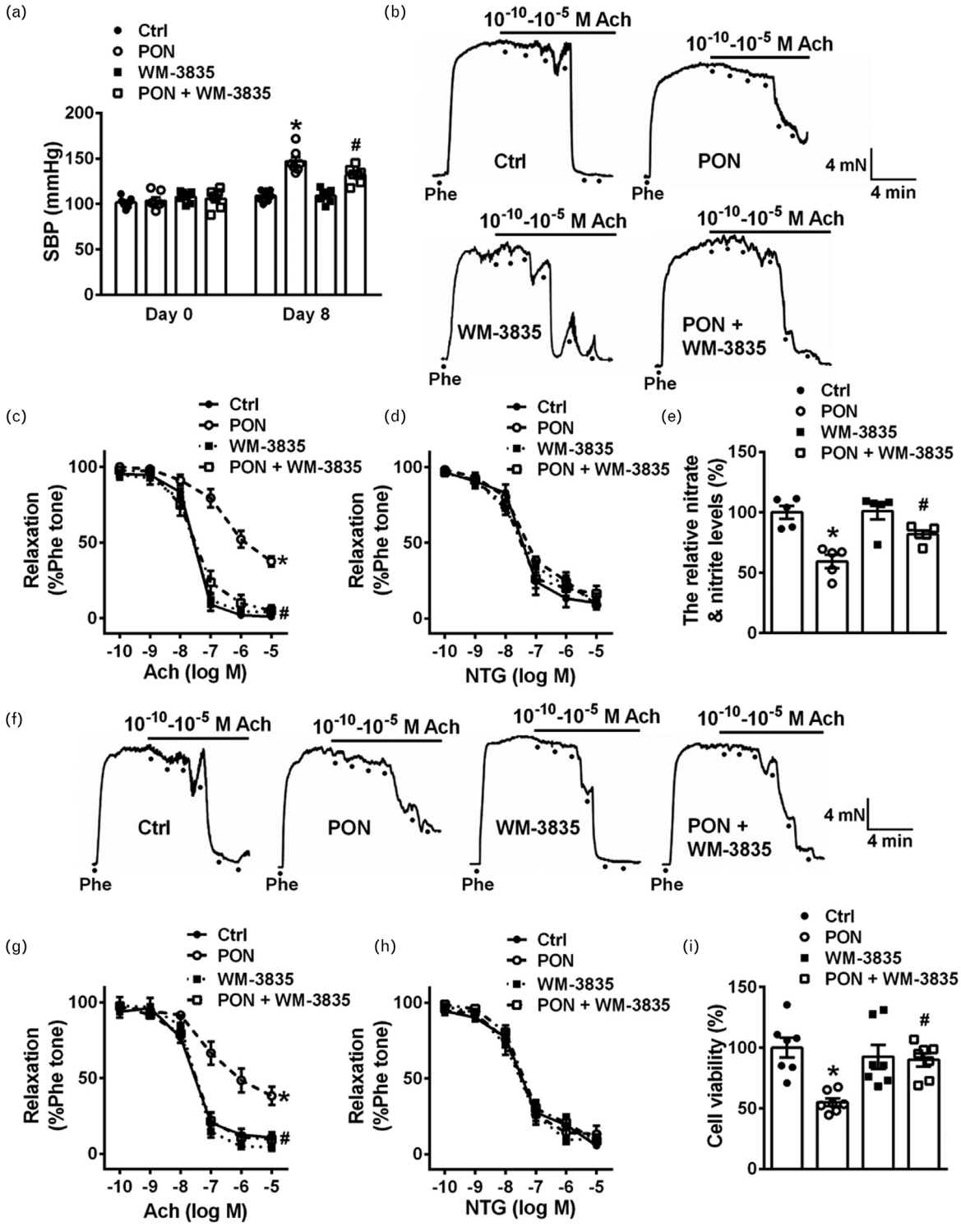

FIGURE 3 Inhibition of KAT7 ameliorates ponatinib-induced hypertension and EDR dysfunction in SD rats. (a) SBP was measured in control and ponatinib administration rats with or without WM-3835 by the noninvasive tail-cuff method. The data are means ± SEM, $n = 7$ per group. $^{*}P < 0.05$ versus control; $^{\#}P < 0.05$ versus ponatinib. (b) Representative traces obtained by wire myography and (c) summarized data of Ach-induced relaxation of the MA rings isolated from the control and ponatinib administration rats with or without WM-3835, followed by precontracting with 10 μM Phe before application of 0.1 nM to 10 μM Ach. The data are means ± SEM, $n = 6$ per group. $^{*}P < 0.05$ versus control; $^{\#}P < 0.05$ ponatinib. (d) Summarized percentage changes of endothelium-independent relaxation in response to different concentrations of NTG (0.1 nM to10 μM) in MA rings from each indicated group (raw data not shown). The data are means ± SEM, $n = 6$ per group. (e) The concentrations of nitrate and nitrite measured in MAs from each indicated group. The data are means ± SEM, $n = 5$ per group. $^{*}P < 0.05$ versus control; $^{\#}P < 0.05$ ponatinib. (f) Representative traces obtained by wire myography and (g) summarized data of Ach-induced relaxation of the MA rings; the rings were under control condition or, respectively, treated with 100 nM ponatinib, 100 nM WM-3835, or 100 nM ponatnib plus 100 nM WM-3835 for 3 h, followed by precontracting with 10 μM Phe before application of 0.1 nM to 10 μM Ach. The data are means ± SEM, $n = 6$ per group. $^{*}P < 0.05$ versus control; $^{\#}P < 0.05$ versus ponatinib. (h) Summarized percentage changes of endothelium-independent relaxation in response to different concentrations of NTG (0.1 nM to 10 μM) in MA rings from each indicated group (raw data not shown). The data are means ± SEM, $n = 6$ per group. (i) Cell viability was measured by CCK-8 in MAECs under control condition or treated with 100 nM ponatinib in the absence or in the presence of 100 nM WM-3835 for 24 h. The data are means ± SEM, $n = 7$ per group. $^{*}P < 0.05$ versus control; $^{\#}P < 0.05$ versus ponatinib.

in the MAs; however, co-treatment with WM-3835 significantly mitigated the EDR dysfunction induced by ponatinib (Fig. 3f, g). Consistent with previous findings, none of the treatments had significant effects on endothelium-independent relaxations in response to NTG (Fig. 3 h). Furthermore, WM-3835 appeared to substantially alleviate endothelial cell damage induced by ponatinib (Fig. 3i). Collectively, the data from both *in vivo* and *in vitro* experiments suggest that the inhibition of KAT7 plays a protective role against ponatinib-induced hypertension and vascular endothelial cells dysfunction.

Inhibition of KAT7 prevents the senescence and inflammation induced by ponatinib

To investigate how KAT7 mediates ponatinib-induced endothelial cell dysfunction, a transient transfection experiment was conducted to overexpress KAT7 in MAECs. The expression levels of KAT7 were dramatically increased in cells transfected with the KAT7 overexpression plasmid, as determined by Western blot assays (Fig. 4a).

Given that ponatinib reduces endothelial cell viability, while WM-3835 reverses this effect, we investigated whether these changes involve apoptosis. To this end, we assessed cell apoptosis by examining the protein expression of the pro-apoptosis factor Bax and the antiapoptosis factor Bcl-2. Interestingly, no significant changes in Bax or Bcl-2 expression were observed in the OE-KAT7 groups compared to the NC group (Fig. 2a–c, Supplemental Digital Content, http://links.lww.com/HJH/C654). Similarly, ponatinib treatment did not significantly affect the expression levels of these apoptosis-related proteins, either in MAs isolated from animals or in MAECs (Fig. 2d–i, Supplemental Digital Content, http://links.lww.com/HJH/C654). Consistently, WM-3835, whether administered alone or in combination with ponatinib, had no effect on BAX or Bcl-2 expression (Fig. 2d–i, Supplemental Digital Content, http://links.lww.com/HJH/C654). These findings suggest that the reduction in endothelial cell viability induced by ponatinib is unlikely to be mediated by apoptosis and may involve alternative mechanism.

Considering that TKIs have been shown to induce cellular senescence, we carried out experiments to investigate the effects of ponatinib and OE-KAT7 on cell fate. The results showed that the number of SA-β-gal positive cells, a marker of cellular senescence, was significantly higher in the OE-KAT7 group compared to the NC group (Fig. 4b). Similarly, the expression of p21, another marker of cellular senescence, was also upregulated in the OE-KAT7 group (Fig. 4c). Senescence cells not only occupy space for the proliferation of new cells but also release inflammatory factors that damage surrounding tissue. Therefore, we focused on the alterations of IL-6 and IL-8, the main inflammatory factors released from senescence cells. The results indicated that OE-KAT7 elevated levels of both IL-6 and IL-8 compared to the NC group (Fig. 4d). These finding demonstrate that KAT7 promotes the senescence and inflammation in MAECs.

To determine whether KAT7-induced senescence and inflammation involves in the vascular endothelial dysfunction induced by ponatinib, a series of experiments were performed. Our results demonstrated that ponatinib significantly increased the number of the SA-β-gal positive cells in MAECs (Fig. 4e, f). Furthermore, ponatinib administration in SD rats led to an increase in p21 protein expression in MAs (Fig. 4g). Similar results were obtained in MAECs treated with ponatinib (Fig. 4h). Notably, WM-3835 markedly reduced the senescence phenotype, as indicated by a decrease in the number SA-β-gal positive cells and p21 protein expression (Fig. 4e-h).

Moreover, we observed that ponatinib induced inflammation, as evidenced by the increased expression of IL-6 and IL-8 in MA of ponatinib-treated SD rats and in MAECs exposed to ponatinib (Fig. 4i, j). These findings were consistent with the effects observed with OE-KAT7. Interestingly, WM-3835 markedly attenuated the elevated levels of IL-6 and IL-8 induced by ponatinib (Fig. 4i, j). In summary, the enhancement of KAT7 expression mediates vascular endothelial senescence and inflammation associated with ponatinib, potentially contributing to the endothelial damage induced by ponatinib.

KAT7 enhances p21 transcription through H3K14 acetylation

To investigate the role of KAT7 in mediating senescence in MAECs, we examined histone modifications, specifically H3 lysine 14 acetylation (H3K14ac) and H3 lysine 23 acetylation (H3K23ac), the substrates of KAT7 [19,27]. Our results demonstrated that OE-KAT7 significantly increased H3K14ac levels, while changes in H3K23ac were not statistically significant (Fig. 5a–c). Furthermore, ponatinib administration in SD rats elevated H3K14ac levels, an effect that was inhibited by WM-3835 (Fig. 5d–f). Similar trends were observed in MAECs exposed to ponatinib and WM-3835 (Fig. 5g–i), suggesting that H3K14ac may serve as a specific substrate for KAT7 in these cells. To further explore the mechanism, we employed chromatin immunoprecipitation followed by quantitative polymerase chain reaction (ChIP-qPCR) and found that KAT7 overexpression promoted its binding to the p21 promoter region (Fig. 5j). Notably, the increased H3K14ac levels induced by OE-KAT7 were associated with upregulated p21 transcription (Fig. 5j). These findings collectively suggest that KAT7 promotes p21 expression through H3K14 acetylation.

Inhibition of KAT7 ameliorates ponatinib-induced cellular senescence and inflammation by blocking nuclear factor-κB cascade

To investigate the mechanisms by which ponatinib triggers inflammation via increasing KAT7 expression, we examined the role of the transcription factor NF-κB, a key mediator of the inflammatory response [28]. Initially, we observed an increase in phosphorylated p65 levels in OE-KAT7 MAECs compared with the NC group (Fig. 6a), indicating the activation of NF-κB.

To further validate this, we isolated MAs from SD rats administered ponatinib and found that the levels of phosphorylated p65 were also increased in these MAs compared to the control group (Fig. 6b). However, WM-3835 significantly reversed the elevated phosphorylated p65 levels induced by ponatinib (Fig. 6b). Similar patterns were observed in MAECs treated with ponatinib and WM-3835

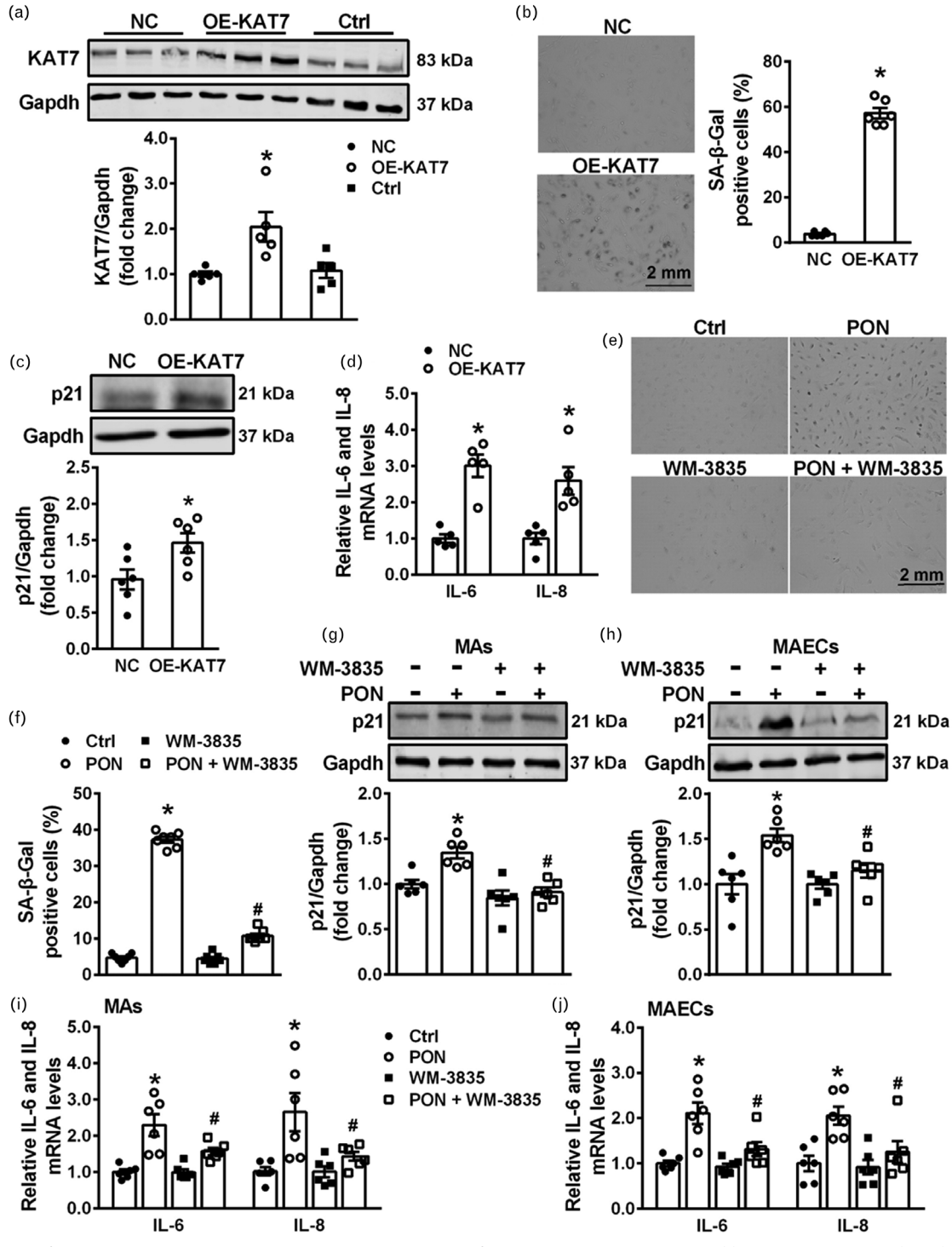

FIGURE 4 Inhibition of KAT7 attenuates the vascular endothelial senescence and inflammation induced by ponatinib. (a) Western blot analysis (upper) and summarized data (lower) of KAT7 expression in MAECs under transiently transfected with either OE-KAT7 plasmid or the corresponding vector plasmid. The data are means ± SEM, $n = 5$ per group. $^{*}P < 0.05$ versus NC. (b) Representative bright field images (left) show SA-β-gal positive cells stained in blue and summary data (right) are expressed as percentage of SA-β-gal positive cells. The data are means ± SEM, $n = 6$ per group. $^{*}P < 0.05$ versus NC. (c) Western blot analysis (upper) and summarized data (lower) of p21 expression in MAECs under transiently transfected with either OE-KAT7 plasmid or the corresponding vector plasmid. The data are means ± SEM, $n = 6$ per group. $^{*}P < 0.05$ versus NC. (d) IL-6 and IL-8 levels were measured in MAECs under transiently transfected with either OE-KAT7 plasmid or the corresponding vector plasmid by PCR. The data are means ± SEM, $n = 5$ per group. $^{*}P < 0.05$ versus NC. (e) Representative bright field images show SA-β-gal positive cells stained in blue and (f) summary data are expressed as percentage of SA-β-gal positive cells. The data are means ± SEM, $n = 7$ per group.$^{*}P < 0.05$ versus control; $^{\#}P < 0.05$ versus ponatinib. (g) Western blot analysis (upper) and summarized data (lower) of p21 expression in MAs isolated form control and ponatinib administration rats with or without WM-3835. The data are means ± SEM, $n = 6$ per group. $^{*}P < 0.05$ versus control; $^{\#}P < 0.05$ versus ponatinib. (h) Western blot analysis (upper) and summarized data (lower) of p21 expression in MAECs under control condition or treated with 100 nM ponatinib in the absence or in the presence of 100 nM WM-3835 for 24 h. The data are means ± SEM, $n = 6$ per group. $^{*}P < 0.05$ versus control; $^{\#}P < 0.05$ versus ponatinib. (i) IL-6 and IL-8 levels were measured in MAs isolated from control and ponatinib administration rats with or without WM-3835 by PCR. The data are means ± SEM, $n = 6$ per group. $^{*}P < 0.05$ versus control; $^{\#}P < 0.05$ versus ponatinib. (j) IL-6 and IL-8 levels were measured in MAECs under control condition or treated with 100 nM ponatinib in the absence or in the presence of 100 nM WM-3835 for 24 h by PCR. The data are means ± SEM, $n = 6$ per group. $^{*}P < 0.05$ versus control; $^{\#}P < 0.05$ versus ponatinib.

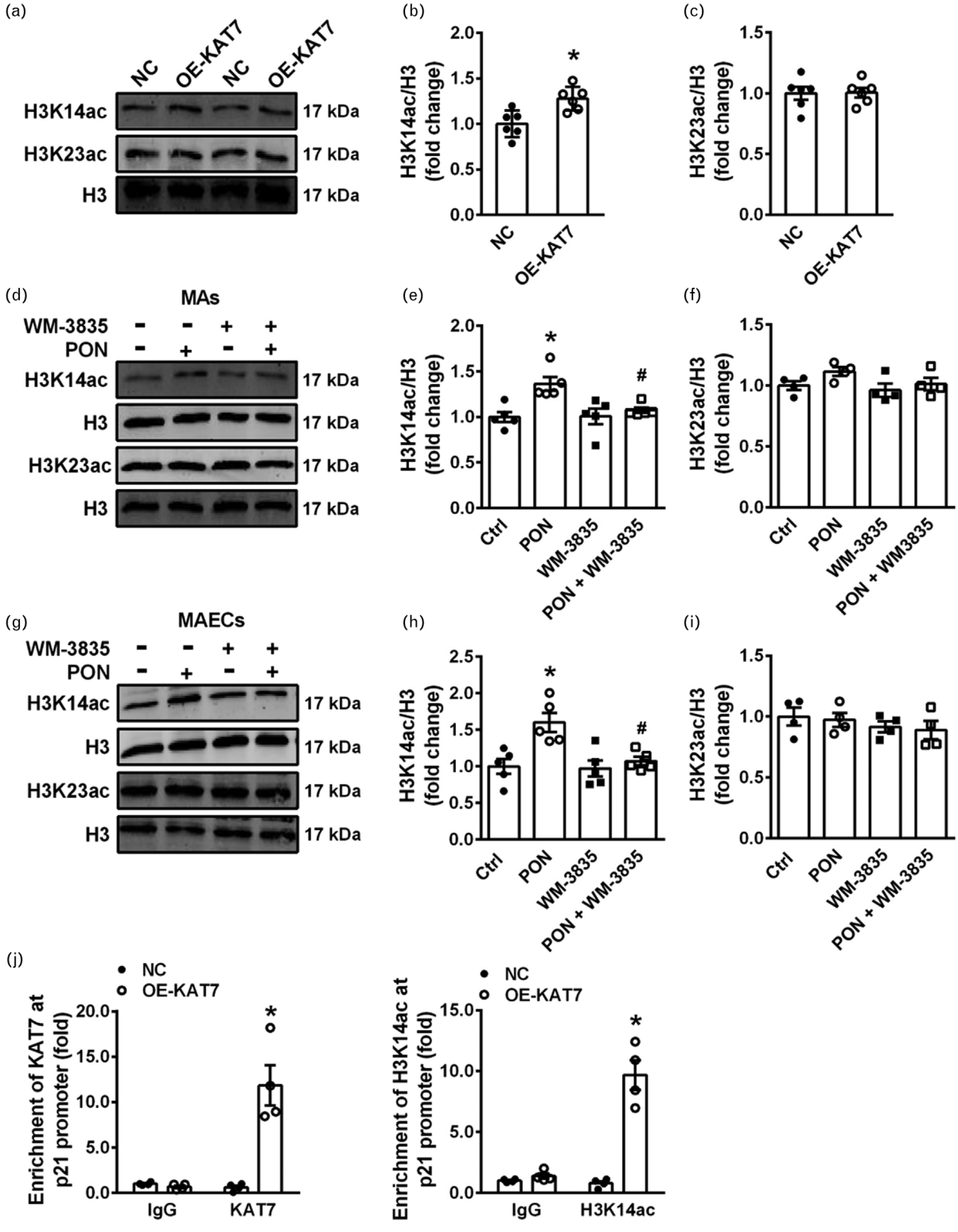

FIGURE 5 KAT7 binds to the promoter region of p21 through H3K14 acetylation. (a) Representative Western blot and (b-c) summarized data showing H3K14ac and H3K23ac expression in MAECs under transiently transfected either OE-KAT7 plasmid or the corresponding vector plasmid. Loading control, histone H3. The data are means ± SEM, $n = 6$ per group. $^{*}P < 0.05$ versus NC. (d) Representative Western blot and (e-f) summarized data showing H3K14ac and H3K23ac protein levels in MAs isolated form control and ponatinib administration rats with or without WM-3835. The data are means ± SEM, $n = 4–5$ per group. $^{*}P < 0.05$ versus control; $^{\#}P < 0.05$ versus ponatinib. (g) Representative Western blot and (h-i) summarized data showing H3K14ac and H3K23ac protein levels in MAECs under control condition or treated with 100 nM ponatinib in the absence or in the presence of 100 nM WM-3835 for 24 h. The data are means ± SEM, $n = 4–5$ per group. $^{*}P < 0.05$ versus control; $^{\#}P < 0.05$ versus ponatinib. (j) Enrichment of KAT7 (left) and H3K14ac (right) in the promoter of the p21 in MAECs under transiently transfected either OE-KAT7 plasmid or the corresponding vector plasmid. $n = 4$ per group. $^{*}P < 0.05$ versus NC.

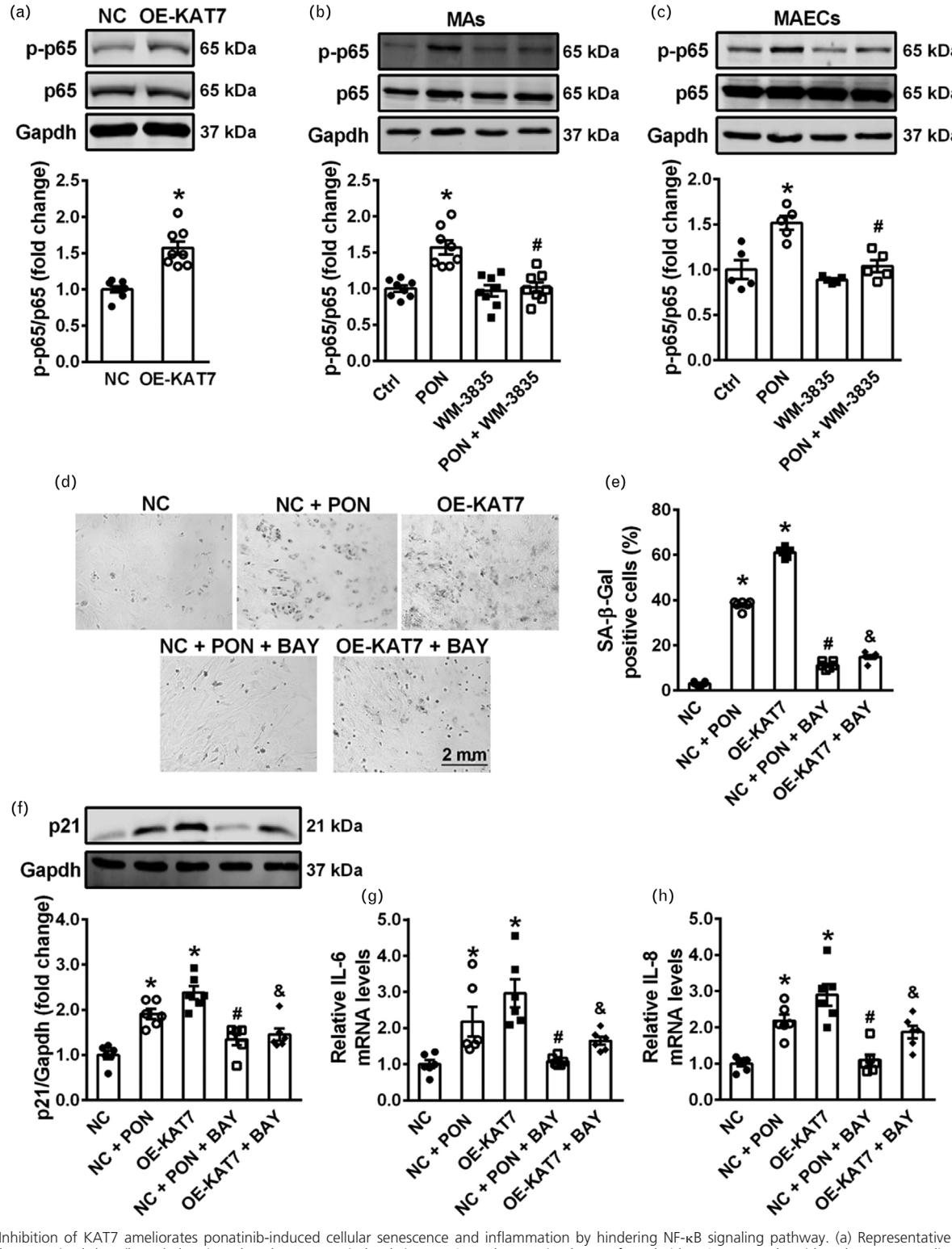

FIGURE 6 Inhibition of KAT7 ameliorates ponatinib-induced cellular senescence and inflammation by hindering NF-κB signaling pathway. (a) Representative Western blot (upper) and summarized data (lower) showing phosph-p65 protein levels in MAECs under transiently transfected either OE-KAT7 plasmid or the corresponding vector plasmid. The data are means ± SEM, $n = 8$ per group. $^{*}P < 0.05$ versus NC. (b) Representative Western blot (upper) and summarized data (lower) showing phosph-p65 protein levels in MAs isolated form control and ponatinib administration rats with or without WM-3835. The data are means ± SEM, $n = 8$ per group. $^{*}P < 0.05$ versus control; $^{\#}P < 0.05$ versus ponatinib. (c) Representative Western blot (upper) and summarized data (lower) showing phosph-p65 protein levels in MAECs under control condition or treated with 100 nM ponatinib in the absence or in the presence of 100 nM WM-3835 for 24 h. The data are means ± SEM, $n = 5$ per group. $^{*}P < 0.05$ versus control; $^{\#}P < 0.05$ versus ponatinib. (d) Representative bright field images show SA-β-gal positive cells stained in blue and (e) summary data are expressed as percentage of SA-β-gal positive cells in MAECs under transiently transfected with either OE-KAT7 plasmid or the corresponding vector plasmid, following exposure to 100 nM ponatinib or 5 μM BAY 11-7085. The data are means ± SEM, $n = 6$ per group.$^{*}P < 0.05$ versus NC; $^{\#}P < 0.05$ versus ponatinib; $^{\&}P < 0.05$ versus OE-KAT7. (f) Representative Western blot (upper) and summarized data (lower) showing p21 in MAECs under the indicated conditions. The data are means ± SEM, $n = 6$ per group. $^{*}P < 0.05$ versus NC, $^{\#}P < 0.05$ versus ponatinib; $^{\&}P < 0.05$ versus OE-KAT7. (g, h) IL-6 and IL-8 levels were measured in MAECs under the indicated conditions. The data are means ± SEM, $n = 6$ per group. $^{*}P < 0.05$ versus NC; $^{\#}P < 0.05$ versus ponatinib; $^{\&}P < 0.05$ versus OE-KAT7.

(Fig. 6c). These findings indicate that the potential of WM-3835 to mitigate NF-κB activation triggered by ponatinib. Importantly, no remarkable difference in total p65 levels were detected among these groups. Collectively, these findings suggest that NF-κB may act as a downstream effector of KAT7 and may contribute to ponatinib-mediated inflammation.

To further investigate the role of NF-κB in ponatinib/OE-KAT7 induced senescence and inflammation, we used a specific inhibitor, BAY 11-7085, to inhibit NF-κB activation in MAECs. BAY 11-7085 led to a reduction in the number of SA-β-gal positive stained cell, as well as a decrease in p21 expression in MAECs subjected to ponatinib or OE-KAT7 (Fig. 6d–f). Moreover, the production of pro-inflammatory cytokines (IL-6 and IL-8) was suppressed by BAY 11-7085 in MAECs treated with ponatinib or OE-KAT7 (Fig. 6g, h). These results suggest that the activation of the NF-κB signaling pathway, mediated by KAT7, is responsible for the cellular senescence and inflammation induced by ponatinib.

DISCUSSION

The major findings of the present study are: ponatinib-induced KAT7 overexpression led to classical features of cellular senescence in MAECs, as demonstrated by impaired cell viability, an increased SA-β-gal-positive cells number, upregulation aging-associated protein p21, and the accumulation of inflammation factors through H3K14 acetylation and activation of NF-κB pathway. These factors ultimately impair EDR and contribute to hypertension (illustrated Fig. 7).

Most clinical trials have demonstrated that vascular endothelial growth factor inhibitors increase blood pressure, with 30–80% of patients developing hypertension [29]. The incidence of hypertension in patients receiving ponatinib, lenvatinib, and sunitinib can reach 68%, 42%, and 21.6%, respectively [7,24,30]. Among these agents, ponatinib appears to be the most likely to induce hypertension. Previous studies indicate that vascular endothelial cells dysfunction may be the primary cause of ponatinib's cardiovascular adverse effects, as it leads to a downregulation of phosphorylated eNOS, inhibition of endothelial survival, endothelial senescence, inflammatory response and endothelial activation [11,31–34]. In our study involving ponatinib-induced hypertension SD rats, we also found that ponatinib significantly impaired EDR, reduced NO generation and caused endothelial damage.

KAT7 has been shown to have a significant positive correlation with human abdominal aortic aneurysm and sprouting angiogenesis [35–37]. However, the specific role of KAT7 in contributing to pathological vascular function, particularly in TKIs-induced vascular toxicity events, remains unclear. In our study, we found that KAT7 is predominantly expressed in vascular endothelial cells and is upregulated by ponatinib. Importantly, inhibiting KAT7 with WM-3835 has a protective effect against ponatinib-induced hypertension, EDR dysfunction and endothelial injury. These data suggest that targeting KAT7 could potentially be served as therapeutic strategy for managing ponatinib-induced vascular toxicity and hypertension.

While previous studies have reported that ponatinib induces cell apoptosis [11,38], our findings suggest otherwise in the context of MAECs. Specifically, we observed no significant changes in the expression of Bax and Bcl-2, key markers of apoptosis, following ponatinib treatment. This discrepancy may be attributed to differences in cell types used across studies. For example, Lv and coworkers have

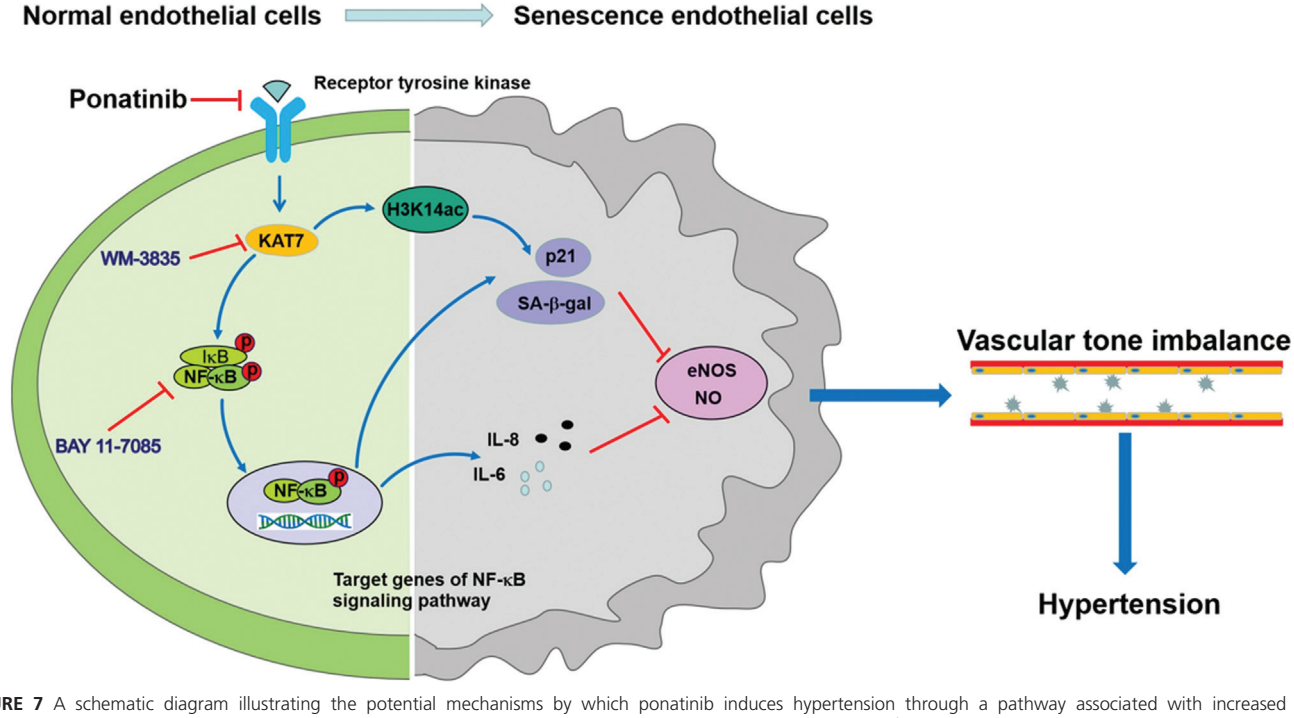

FIGURE 7 A schematic diagram illustrating the potential mechanisms by which ponatinib induces hypertension through a pathway associated with increased KAT7 expression. This increase leads to H3K14 acetylation and NF-κB activation, which mediate cellular senescence and inflammatory responses in vascular endothelial cells.

reported that ponatinib inhibits apoptosis in human type I alveolar epithelial cell [39], highlighting the variability in cellular responses to ponatinib depending on cell type and its physiological state. Similarly, our results showed that WM-3835, either alone or in combination with ponatinib, did not alter Bax and Bcl-2 expression in MAECs. This contrasts with findings from other studies, which reported that WM-3835 induces apoptosis in specific cell types, such as primary human prostate cancer cells derived from castration-resistant prostate cancer patients [27,40]. However, WM-3835 did not induce apoptosis or significant cytotoxicity in primary human prostate epithelial cells [40]. These observations suggest that the response to WM-3835 or ponatinib is highly cell type-specific and may be influenced by the pathological or physiological state of the cells. Furthermore, our findings imply that ponatinib-induced reduction of endothelial cell viability and the improved cell viability by WM-3835 are likely not mediated apoptosis. Future studies should aim to elucidate these alternative pathways to better understand the underlying mechanisms of endothelial cell injury.

KAT7 has been identified as a new epigenetic target for delaying aging and treating aging-associated disorders [19]. However, data regarding its role in the vasculature have not yet been obtained. In our study, OE-KAT7 significantly increased the expression of cellular senescence markers p21 and SA-β-gal in MAECs. It is worth noting that the enhancement of KAT7 also contributes to the ponatinib-induced upregulation of p21 and SA-β-gal, as these effects can be reversed by the KAT7 inhibitor WM-3835. Our findings provide further support for the critical role of KAT7 in regulating histone modifications and mediating senescence. Specifically, we found that OE-KAT7 increases H3K14 acetylation, confirming that H3K14 is a specific substrate for endogenous KAT7. This modification appears to play a pivotal role in senescence-related gene regulation [41]. Notably, OE-KAT7 promoted the binding of KAT7 to the p21 promoter region, a key regulator of cell cycle arrest and senescence. The increased H3K14ac levels induced by OE-KAT7 were accompanied by enhanced enrichment of H3K14ac at the p21 promoter, leading to upregulated p21 transcription. This finding highlights a mechanistic link between KAT7 activity, histone acetylation, and transcriptional activation of senescence-associated genes. Interestingly, ponatinib treatment also selectively increased H3K14ac, but not H3K23ac, suggesting that this histone modification is uniquely associated with the senescence-inducing effects of KAT7 in vascular endothelial cells. Furthermore, the administration of WM-3835, a specific inhibitor of KAT7, effectively abolished the increase in H3K14ac induced by ponatinib, further supporting the specificity of this pathway. Therefore, these results suggest that ponatinib induces senescence in vascular endothelial cells, at least in part, through KAT7-mediated H3K14 acetylation. Given the close association between cellular senescence and damage to vascular endothelial cells [42], we propose that KAT7-mediated senescence may be linked to vascular dysfunction induced by ponatinib.

Previous studies have reported that ponatinib mediates inflammatory responses in cellular models or patients [33,43]. Here, we observed that ponatinib increased the levels of IL-6, IL-8, and phospho-p65 in both *in vivo* and *in vitro* experiments. Cellular senescence not only involves cell cycle progression, but also secretes inflammatory cytokines that contribute to chronic inflammation [44]. IL-6 and IL-8 are particularly key components of SASP [45]. Therefore, we believe that ponatinib-induced inflammation may result from cellular senescence. Importantly, KAT7 plays a crucial role in this process, as evidenced by WM-3835 reversing the upregulation of IL-6, IL-8, and the activation of NF-κB signaling pathway in ponatinib-treated MAECs or animal models of ponatinib-induced hypertension. Additionally, the inhibition of NF-κB with BAY 11-7085 effectively reduces the elevation of senescence markers and the accumulation of IL-6 and IL-8 induced by ponatinib or OE-KAT7 in MAECs, indicating that the KAT7/NF-κB axis plays a role in ponatinib-induced senescence and inflammation. Overall, KAT7 is associated with senescence and inflammatory responses, suggesting that inhibition of KAT7 to mitigate ponatinib-induced hypertension and vasotoxicity may involve downregulating the senescence process and reducing inflammation.

The prevention and management of TKIs-related adverse cardiovascular events become increasingly important, given the widespread use of these agents to improve patient survival and delay tumor progression [10,46–48]. Recent studies conducted by our research group have elucidated the signaling mechanisms underlying TKIs-induced hypertension. Aflibercept, sunitinib, and lenvatinib all induce hypertension by impairing endothelial cell function through various mechanisms, including the inhibition of the CAT-1/Akt/eNOS signaling pathway, IRS-1- and Pellino-1-mediated inhibition of AKT/eNOS signaling, and endothelial ferroptosis [24,30,49]. Our findings regarding the detrimental effects of ponatinib on endothelial cells are consistent with previous reports. However, ponatinib may increase KAT7 expression, which activates NF-κB signaling pathway, promoting senescence and releasing inflammatory cytokines, ultimately resulting in vascular dysfunction and hypertension. Based on these findings, the mechanisms underlying vascular toxicity/hypertension caused by TKIs differ, potentially due to their multiple targets on endothelial cells.

WM-3835, a potent inhibitor of KAT7, has demonstrated effective antitumor effects both *in vitro* and *in vivo* [50]. Our data indicate that WM-3835 plays a protective role against ponatinib-induced hypertension. This dual effect of WM-3835 suggests that, in the treatment of specific tumors such as acute myeloid leukemia and prostate cancer, the combined use of ponatinib and KAT7 inhibitors may yield greater clinical benefits. However, further clinical research is necessary for validation.

In summary, our study describes the potential mechanism underlying ponatinib-induced hypertension using a rat model, which involves KAT7-mediated endothelial senescence and inflammation through acetylation H3K14 and activation of NF-κB signaling. These findings offer a theoretical foundation for future clinical research.

ACKNOWLEDGEMENTS

This work was generously supported by grants from the National Natural Science Foundation of China (Nos. 81870370, 81930009, and 82230008 to Zhi-Ren Zhang;

81700367 to Liang-Liang Tang; 81800513 to Chang-Jiang Yu). Outstanding Youth Fund (No. JCQN2020-02 to Chang-Jiang Yu), and Nn10 program of Harbin Medical University Cancer Hospital (to Zhi-Ren Zhang).

Authorship contribution statement: Liang-Liang Tang and Zhi-Ren Zhang were responsible for the major conception and design of the study. Xin-Yu Xu, Mei Zhang, Qi Qin, Rong-Xue, Shuai Jiang, Xu Yang carried out experiments; Liang-Liang Tang, Chen-Liang, Qiu-Shi Wang analyzed data and prepared figures; Liang-Liang Tang, Qi Qin, Chang-Jiang Yu and Zhi-Ren Zhang drafted and revised the manuscript; all authors approved the final version of the manuscript.

Conflicts of interest

The authors declare that they have no competing interests.

REFERENCES

1. Levy MY, McGarry LJ, Huang H, Lustgarten S, Chiroli S, Iannazzo S. Benefits and risks of ponatinib versus bosutinib following treatment failure of two prior tyrosine kinase inhibitors in patients with chronic phase chronic myeloid leukemia: a matching-adjusted indirect comparison. *Curr Med Res Opin* 2019; 35:479–487.
2. Sacha T, Szczepanek E, Dumnicka P, Góra-Tybor J, Niesiobędzka-Krężel J, Prejzner W, *et al.* The outcomes of ponatinib therapy in patients with chronic myeloid leukemia resistant or intolerant to previous tyrosine kinase inhibitors, treated in Poland within the donation program. *Clin Lymphoma Myeloma Leuk* 2022; 22:405–415.
3. Gozgit JM, Wong MJ, Moran L, Wardwell S, Mohemmad QK, Narasimhan NI, *et al.* Ponatinib (AP24534), a multitargeted pan-FGFR inhibitor with activity in multiple FGFR-amplified or mutated cancer models. *Mol Cancer Ther* 2012; 11:690–699.
4. Chang HM, Moudgil R, Scarabelli T, Okwuosa TM, Yeh ETH. Cardiovascular complications of cancer therapy: best practices in diagnosis, prevention, and management: part 1. *J Am Coll Cardiol* 2017; 70:2536–2551.
5. Cortes J, Apperley J, Lomaia E, Moiraghi B, Undurraga Sutton M, Pavlovsky C, *et al.* Ponatinib dose-ranging study in chronic-phase chronic myeloid leukemia: a randomized, open-label phase 2 clinical trial. *Blood* 2021; 138:2042–2050.
6. Zeng P, Schmaier A. Ponatinib and other CML tyrosine kinase inhibitors in thrombosis. *Int J Mol Sci* 2020; 21:.
7. Chang HM, Okwuosa TM, Scarabelli T, Moudgil R, Yeh ETH. Cardiovascular complications of cancer therapy: best practices in diagnosis, prevention, and management: part 2. *J Am Coll Cardiol* 2017; 70:2552–2565.
8. Cortes JE, Kim DW, Pinilla-Ibarz J, le Coutre PD, Paquette R, Chuah C, *et al.* Ponatinib efficacy and safety in Philadelphia chromosome-positive leukemia: final 5-year results of the phase 2 PACE trial. *Blood* 2018; 132:393–404.
9. Agarwal M, Thareja N, Benjamin M, Akhondi A, Mitchell GD. Tyrosine kinase inhibitor-induced hypertension. *Curr Oncol Rep* 2018; 20:65.
10. Luciano L, Annunziata M, Attolico I, Di Raimondo F, Maggi A, Malato A, *et al.* The multityrosine kinase inhibitor ponatinib for chronic myeloid leukemia: Real-world data. *Eur J Haematol* 2020; 105:3–15.
11. Madonna R, Pieragostino D, Cufaro MC, Doria V, Del Boccio P, Deidda M, *et al.* Ponatinib induces vascular toxicity through the notch-1 signaling pathway. *J Clin Med* 2020; 9:.
12. Deng QF, Li C, Liu J, Ji XX, Wan XY, Wang CY, *et al.* DNMT3A governs tyrosine kinase inhibitors responses through IAPs and in a cell senescence-dependent manner in nonsmall cell lung cancer. *Am J Cancer Res* 2023; 13:3517–3530.
13. Procopio MG, Laszlo C, Al Labban D, Kim DE, Bordignon P, Jo SH, *et al.* Combined CSL and p53 downregulation promotes cancer-associated fibroblast activation. *Nat Cell Biol* 2015; 17:1193–1204.
14. Madonna R, Pieragostino D, Cufaro MC, Del Boccio P, Pucci A, Mattii L, *et al.* Sex-related differential susceptibility to ponatinib cardiotoxicity and differential modulation of the Notch1 signalling pathway in a murine model. *J Cell Mol Med* 2022; 26:1380–1391.
15. Madonna R, Barachini S, Moscato S, Ippolito C, Mattii L, Lenzi C, *et al.* Sodium-glucose cotransporter type 2 inhibitors prevent ponatinib-induced endothelial senescence and disfunction: a potential rescue strategy. *Vascul Pharmacol* 2022; 142:106949.
16. Huang W, Hickson LJ, Eirin A, Kirkland JL, Lerman LO. Cellular senescence: the good, the bad and the unknown. *Nat Rev Nephrol* 2022; 18:611–627.
17. Kumari R, Jat P. Mechanisms of cellular senescence: cell cycle arrest and senescence associated secretory phenotype. *Front Cell Dev Biol* 2021; 9:645593.
18. Bloom SI, Islam MT, Lesniewski LA, Donato AJ. Mechanisms and consequences of endothelial cell senescence. *Nat Rev Cardiol* 2023; 20:38–51.
19. Wang W, Zheng Y, Sun S, Li W, Song M, Ji Q, *et al.* A genome-wide CRISPR-based screen identifies KAT7 as a driver of cellular senescence. *Sci Transl Med* 2021; 13:.
20. Zheng WV, Xu W, Li Y, Qin J, Zhou T, Li D, *et al.* Antiaging effect of **β**-carotene through regulating the KAT7-P15 signaling axis, inflammation and oxidative stress process. *Cell Mol Biol Lett* 2022; 27:86.
21. Yang Y, Kueh AJ, Grant ZL, Abeysekera W, Garnham AL, Wilcox S, *et al.* The histone lysine acetyltransferase HBO1 (KAT7) regulates hematopoietic stem cell quiescence and self-renewal. *Blood* 2022; 139:845–858.
22. Wang B, Li J, Liu L, Song G. Insulin sensitivity in the aged heart is improved by down-regulation of KAT7 in vivo and in vitro. *Cell Cycle* 2022; 21:276–288.
23. McGrath JC, Drummond GB, McLachlan EM, Kilkenny C, Wainwright CL. Guidelines for reporting experiments involving animals: the ARRIVE guidelines. *Br J Pharmacol* 2010; 160:1573–1576.
24. Liu Y, Tang LL, Liang C, Wu MM, Zhang ZR. Insulin resistance and pellino-1 mediated decrease in the activities of vasodilator signaling contributes to sunitinib-induced hypertension. *Front Pharmacol* 2021; 12:617165.
25. Tang LL, Yang X, Yu SQ, Qin Q, Xue R, Sun Y, *et al.* Aldosterone-stimulated endothelial epithelial sodium channel (EnNaC) plays a role in cold exposure-induced hypertension in rats. *Front Pharmacol* 2022; 13:970812.
26. Liu HB, Zhang J, Sun YY, Li XY, Jiang S, Liu MY, *et al.* Dietary salt regulates epithelial sodium channels in rat endothelial cells: adaptation of vasculature to salt. *Br J Pharmacol* 2015; 172:5634–5646.
27. Wang H, Qiu Y, Zhang H, Chang N, Hu Y, Chen J, *et al.* Histone acetylation by HBO1 (KAT7) activates Wnt/**β**-catenin signaling to promote leukemogenesis in B-cell acute lymphoblastic leukemia. *Cell Death Dis* 2023; 14:498.
28. Liu T, Zhang L, Joo D, Sun SC. NF-**κ**B signaling in inflammation. *Signal Transduct Target Ther* 2017; 2:17023.
29. Touyz RM, Herrmann SMS, Herrmann J. Vascular toxicities with VEGF inhibitor therapies-focus on hypertension and arterial thrombotic events. *J Am Soc Hypertens* 2018; 12:409–425.
30. Liang C, Zhu D, Xia W, Hong Z, Wang QS, Sun Y, *et al.* Inhibition of YAP by lenvatinib in endothelial cells increases blood pressure through ferroptosis. *Biochim Biophys Acta Mol Basis Dis* 2023; 1869:166586.
31. Haguet H, Bouvy C, Delvigne AS, Modaffari E, Wannez A, Sonveaux P, *et al.* The risk of arterial thrombosis in patients with chronic myeloid leukemia treated with second and third generation bcr-abl tyrosine kinase inhibitors may be explained by their impact on endothelial cells: an in-vitro study. *Front Pharmacol* 2020; 11:1007.
32. Yu B, Osman AEG, Sladojevic N, Prabhu N, Tai HC, Chen D, *et al.* Involvement of rho-associated coiled-coil containing kinase (ROCK) in BCR-ABL1 tyrosine kinase inhibitor cardiovascular toxicity. *JACC CardioOncol* 2022; 4:371–383.
33. Paez-Mayorga J, Chen AL, Kotla S, Tao Y, Abe RJ, He ED, *et al.* Ponatinib activates an inflammatory response in endothelial cells via ERK5 SUMOylation. *Front Cardiovasc Med* 2018; 5:125.
34. Ai N, Chong CM, Chen W, Hu Z, Su H, Chen G, *et al.* Ponatinib exerts antiangiogenic effects in the zebrafish and human umbilical vein endothelial cells via blocking VEGFR signaling pathway. *Oncotarget* 2018; 9:31958–31970.
35. Yan MS, Turgeon PJ, Man HJ, Dubinsky MK, Ho JJD, El-Rass S, *et al.* Histone acetyltransferase 7 (KAT7)-dependent intragenic histone acetylation regulates endothelial cell gene regulation. *J Biol Chem* 2018; 293:4381–4402.
36. Grant ZL, Hickey PF, Abeysekera W, Whitehead L, Lewis SM, Symons RCA, *et al.* The histone acetyltransferase HBO1 promotes efficient tip cell sprouting during angiogenesis. *Development* 2021; 148:.
37. Han Y, Tanios F, Reeps C, Zhang J, Schwamborn K, Eckstein HH, *et al.* Histone acetylation and histone acetyltransferases show significant alterations in human abdominal aortic aneurysm. *Clin Epigenetics* 2016; 8:3.

38. Krajcsir B, Pócsi M, Fejes Z, Nagy B Jr, Kappelmayer J, Beke Debreceni I. Ponatinib induces a procoagulant phenotype in human coronary endothelial cells via inducing apoptosis. *Pharmaceutics* 2024; 16:.
39. Qu Y, Zhang L, Kang Z, Jiang W, Lv C. Ponatinib ameliorates pulmonary fibrosis by suppressing TGF-β1/Smad3 pathway. *Pulm Pharmacol Ther* 2015; 34:1–7.
40. Mi YY, Ji Y, Zhang L, Sun CY, Wei BB, Yang DJ, *et al.* A first-in-class HBO1 inhibitor WM-3835 inhibits castration-resistant prostate cancer cell growth in vitro and in vivo. *Cell Death Dis* 2023; 14:67.
41. Zhang F, Icyuz M, Bartke A, Sun LY. The effects of early-life growth hormone intervention on tissue specific histone H3 modifications in long-lived Ames dwarf mice. *Aging (Albany NY)* 2020; 13:1633–1648.
42. Suda M, Paul KH, Minamino T, Miller JD, Lerman A, Ellison-Hughes GM, *et al.* Senescent cells: a therapeutic target in cardiovascular diseases. *Cells* 2023; 12:.
43. Lee EQ, Muzikansky A, Duda DG, Gaffey S, Dietrich J, Nayak L, *et al.* Phase II trial of ponatinib in patients with bevacizumab-refractory glioblastoma. *Cancer Med* 2019; 8:5988–5994.
44. Mehdizadeh M, Aguilar M, Thorin E, Ferbeyre G, Nattel S. The role of cellular senescence in cardiac disease: basic biology and clinical relevance. *Nat Rev Cardiol* 2022; 19:250–264.
45. Vernot JP. Senescence-associated pro-inflammatory cytokines and tumor cell plasticity. *Front Mol Biosci* 2020; 7:63.
46. Abdelmagid MG, Al-Kali A, Litzow MR, Begna KH, Hogan WJ, Patnaik MS, *et al.* Real-world experience with ponatinib therapy in chronic phase chronic myeloid leukemia: impact of depth of response on survival and prior exposure to nilotinib on arterial occlusive events. *Blood Cancer J* 2023; 13:122.
47. Gao Y, Ding Y, Tai XR, Zhang C, Wang D. Ponatinib: an update on its drug targets, therapeutic potential and safety. *Biochim Biophys Acta Rev Cancer* 2023; 1878:188949.
48. Cirmi S, El Abd A, Letinier L, Navarra M, Salvo F. Cardiovascular toxicity of tyrosine kinase inhibitors used in chronic myeloid leukemia: an analysis of the FDA Adverse Event Reporting System Database (FAERS). *Cancers (Basel)* 2020; 12:.
49. Dong ZC, Wu MM, Zhang YL, Wang QS, Liang C, Yan X, *et al.* The vascular endothelial growth factor trap aflibercept induces vascular dysfunction and hypertension via attenuation of eNOS/NO signaling in mice. *Acta Pharmacol Sin* 2021; 42:1437–1448.
50. White J, Derheimer FA, Jensen-Pergakes K, O'Connell S, Sharma S, Spiegel N, *et al.* Histone lysine acetyltransferase inhibitors: an emerging class of drugs for cancer therapy. *Trends Pharmacol Sci* 2024; 45:243–254.